Readers Insight
Publisher of open access books and journals
PJMLS OPEN ACCESS
Print ISSN: 2707-4471. Online ISSN: 2707-448X

Research Article	Pak-Euro Journal of Medical and Life Sciences
DOI: 10.31580/pjmls.v8i4.3405	Copyright © All rights are reserved by Corresponding Author
Vol. 8 No. 4, 2025: pp. 897-912	
www.readersinsight.net/pjmls	**Revised:** October 26, 2025 **Accepted:** October 30, 2025
Submission: September 04, 2025	**Published Online:** December 31, 2025

IN SILICO MOLECULAR INTERACTIONS OF PHENYL ALKYL CAFFEINE DERIVATIVES AS MONOAMINE OXIDASE B INHIBITORS

Uzma Jabeen[1]*, Ayesha Farooq[1], Sumreen Begum[2]*, Tehreem Fatima[3]

[1]**Department of Biochemistry,** Federal Urdu University of Arts, Science and Technology, Gulshan-e-Iqbal, Karachi, Pakistan
[2]**Stem Cell Research Laboratory,** Sindh Institute of Urology and Transplantation, Karachi, Pakistan
[3]**Liaquat College of Medicine and Dentistry,** Karachi, Pakistan
***Corresponding Authors:** Uzma Jabeen. E. mail: dr.uzmajabeen@fuuast.edu.pk and Sumreen Begum. E. mail: sumreenbegum@gmail.com

Abstract

Background: *Neurodegenerative disorders often involve increased monoamine oxidase B (MAO-B) activity, which leads to excessive reactive oxygen species (ROS) and cell damage. Neuroprotection through ROS inhibition can be achieved with MAO-B inhibitors, helping to reduce motor symptoms in Parkinson's disease, amyloid plaques in Alzheimer's disease, and impairment in non-motor issues such as mood, cognition, sleep, and fatigue.*

Methods: *This study investigated the interaction and inhibitory potential of C8-substituted phenyl alkyl caffeine derivatives against monoamine oxidase B (MAO-B) using molecular docking. Docking was performed through the Virtual Screening interface of PyRx, integrated with the AutoDock Vina engine, to evaluate binding affinity and active-site interactions. Additionally, in-silico absorption, distribution, metabolism, and excretion (ADME) profiling and drug-likeness assessments were conducted to determine their suitability as potential reversible MAO-B inhibitors.*

Results: *Caffeine analogs with shorter substituents (4a, 4b) showed moderate interactions with the amino acids in the substrate cavity of MAO-B, whereas derivatives with longer substituents, 8-(5-Phenylpentyl) caffeine (4d), (4e), and (4f), exhibited robust binding affinities, -10.3, -10.5, and -10.3 kcal/mol, respectively. Among these compounds, 4d emerged as the most selective inhibitor, forming strong, stable conventional hydrogen bonds. 4e and 4f also exhibited substantial binding energies. 4i displayed strong interactions with slightly lower efficacy. ADME analysis revealed 4f with high gastrointestinal (GI) absorption and blood-brain barrier (BBB) permeability, suggesting potential for CNS-targeted applications.*

Conclusion: *This study demonstrates that 8-(5-Phenylpentyl) caffeine (4d) and 8-(5-Phenylpentyl) caffeine (4e) are highly selective and potent inhibitors of MAO-B. Among all ligands, 8-(7-Phenylheptyl) caffeine (4f) stood out as a reversible inhibitor, having high GI and BBB permeability. These findings highlight the importance of designing selective and multifunctional MAO-B inhibitors for effective neuroprotective therapy.*

Keywords: *Flavin adenine cofactor, Molecular docking, Monoamine oxidase inhibition, Parkinson's disease, Phenyl alkyl caffeine derivatives, Reversible inhibition*

INTRODUCTION

Monoamine oxidase B (MAO-B) is a crucial enzyme implicated in neurodegenerative diseases such as Parkinson's disease (PD) and Alzheimer's disease (AD), associated with dysregulation of signaling pathways (1). It catalyzes the neurotransmitters such as dopamine, norepinephrine, and serotonin, thereby regulating their synaptic concentrations and maintaining neural homeostasis. By oxidizing them, MAO-B ensures proper brain function and mental health. Dysregulated MAO-B activity contributes to neurological and psychiatric disorders by disrupting neurotransmitter balance and enhancing oxidative stress. Elevated MAO-B activity increases hydrogen peroxide production, leading to the generation of reactive oxygen species (ROS) and neuronal damage (2–4). For instance, PD is characterized by dopaminergic neuronal loss in the substantia nigra pars compacta, partially attributed to altered MAO-B activity (5).

MAO-B inhibitors provide neuroprotection by reducing ROS formation and preserving dopaminergic neurons. These inhibitors improve motor function in PD, reduce amyloid plaque deposition

in AD, and alleviate non-motor symptoms such as mood disturbance, cognitive impairment, and sleep disturbances. Selegiline, rasagiline, and safinamide are the principal MAO-B inhibitors in clinical use; the first two act irreversibly, whereas safinamide binds reversibly (6–9). Selegiline improves motor performance and quality of life in PD patients (10), while rasagiline delays disability progression in multiple system atrophy (11). However, more potent and selective reversible inhibitors are needed to minimize side effects associated with irreversible inhibition (12-15).

Natural products (NPs) such as flavonoids, xanthones, phenolic derivatives, alkaloids, and caffeine have shown promise as sources of MAO-B inhibitors (12, 13). Caffeine, a natural stimulant present in coffee, tea, and cocoa, modulates neurochemical pathways via phosphodiesterase inhibition (16), benzodiazepine receptor binding (17), and MAO-B interaction. Several C8-substituted caffeine derivatives, (E)-8-(3-chlorostyryl) caffeine and 8-(3-bromobenzyloxy) caffeine, exhibit potent MAO-B inhibition with IC_{50} values of 0.128 μM and 0.068 μM, respectively (18, 19). A C8-substituted caffeine analog bearing a 4-phenylbutadien moiety demonstrated dual inhibition of MAO-B and A_2A adenosine receptors, suggesting synergistic neuroprotective effects (20). The structures of reported caffeine derivatives, along with other important inhibitors such as rasagiline, safinamide, and selegiline, are provided in Fig. 1.

Recently, novel reversible and highly selective MAO-B inhibitors have been identified through in silico and medicinal chemistry approaches, characterized by their high reversibility, selectivity, and diminished incidence of adverse effects. Examples include dolutegravir, a dual MAO-B and AChE inhibitor proposed for AD therapy (21), and newly synthesized pyridazinone (TR1–TR16) (22) and nitro-amide (NEA1–NEA5) scaffolds (23).

Structurally, MAO-B exists as a dimer, with each monomer containing a flavin adenine dinucleotide (FAD) cofactor within its active site (24). The enzyme's catalytic pocket comprises two cavities —a substrate cavity and a hydrophobic entrance cavity separated by gating residues Ile199 and Tyr326, which regulate substrate and inhibitor access (25–27). Residue Cys172 further contributes to MAO-B selectivity (28). Structural studies reveal that potent inhibitors typically engage FAD and critical residues such as Ile199, Tyr326, Tyr398, and Tyr435 within the active site (23, 24, 29, 30).

This study aimed to identify potential reversible MAO-B inhibitors among C8-substituted caffeine derivatives through molecular docking (PyRx + AutoDock Vina) and in silico absorption, distribution, metabolism, and excretion (ADME) analyses. To achieve this, we conducted a series of computational docking analyses. The structure of phenyl-alkyl caffeine analogs is given in Table 1. Computational docking was performed to elucidate binding modes and molecular interactions between potent caffeine analogues and the MAO-B active site. ADME profiling was further conducted to predict pharmacokinetic properties such as gastrointestinal absorption (GI), blood–brain barrier (BBB) permeability, and favorable solubility, specifically assessing properties of the synthesized C8-positioned phenyl alkyl caffeine derivatives. These evaluations are intended to support the design of selective, reversible MAO-B inhibitors with optimal neuroprotective potential for managing neurodegenerative diseases.

METHODOLOGY

CHEMICAL COMPOUND PREPARATION

Caffeine analogs were created using ChemSketch software. These eight caffeine analogs were subsequently saved in a mol. file format for future use.

PROTEIN DATA RETRIEVAL AND PROTEIN STRUCTURE REFINEMENT

The crystallographic structure of MAO-B was obtained from the Protein Data Bank (PDB) using the PDB ID (2V5Z) (25, 31). The crystallographic structures were chosen from homo-sapiens showcased optimal ligand enrichment factors (32, 33).

Discovery Studio 2021 Client software was utilized to refine the protein structure (34). It involves the removal of attached ligands, cofactor FAD, and water molecules, and polar hydrogen atoms were introduced. From the two available chains of MAO-B, chain 'A' was selected, and the resulting protein structure was saved in PDB format.

Table I. Chemical and physical data of the titled compounds

S. no.	Name of the compound	Molecular formula	Structure
1.	8-(2-Phenylethyl) caffeine (4a)	$C_{16}H_{18}N_4O_2$	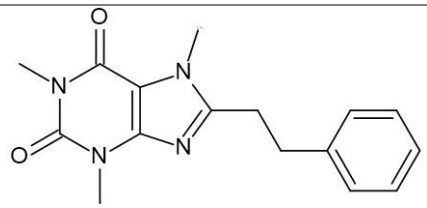
2.	8-(3-Phenylpropyl) caffeine (4b)	$C_{17}H_{20}N_4O_2$	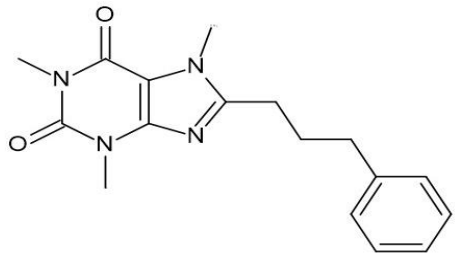
3.	8-(4-Phenylbutyl) caffeine (4c)	$C_{18}H_{22}N_4O_2$	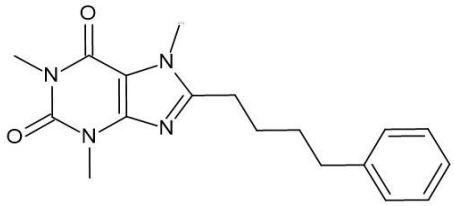
4.	8-(5-Phenylpentyl) caffeine (4d)	$C_{19}H_{24}N_4O_2$	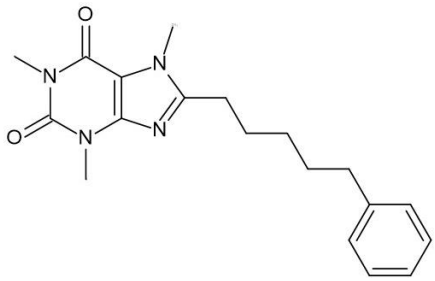
5.	8-(6-Phenylhexyl) caffeine (4e)	$C_{20}H_{26}N_4O_2$	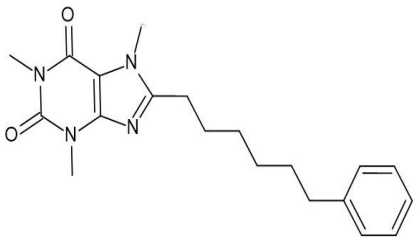
6.	8-(7-Phenylheptyl) caffeine (4f)	$C_{21}H_{28}N_4O_2$	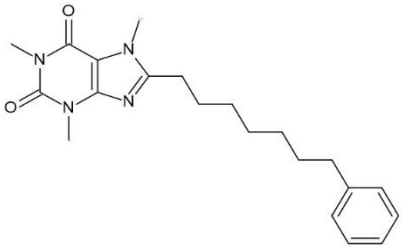
7.	8-(3-Oxo-3-phenylpropyl) caffeine (4h)	$C_{17}H_{18}N_4O_3$	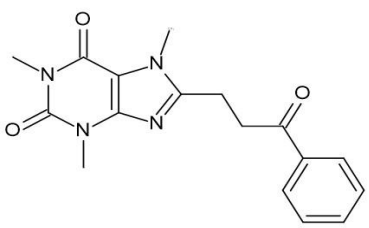
8.	8-(4-Oxo-4-phenylbutyl) caffeine (4i)	$C_{18}H_{22}N_4O_3$	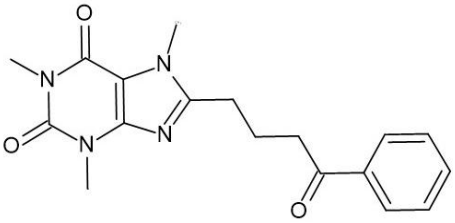

DOCKING ANALYSIS

Docking analysis was conducted using the Virtual Screening software interface PyRx. The protein structure was initially uploaded and converted into pdbqt format by selecting the "make macromolecule" option. Ligands were imported using the Open Babel option, and their energies were minimized. All ligands were then converted into pdbqt format. To specify the active site of MAO-B, the positioning of the grid box was arranged to encompass the entire binding site and facilitate the proper docking of larger molecules. The docking grid box was configured to fully encompass the active site of MAO-B with these parameters: Center coordinates (x = 52.768, y = 154.818, z = 25.920), Grid box dimensions (x = 40 Å, y = 50 Å, z = 40 Å), and exhaustiveness parameter set to 8. These parameters ensured adequate coverage of the enzyme's binding pocket, allowing accurate docking and interaction analysis of the caffeine derivatives. Subsequently, the docking process was initiated by selecting both the ligands and the protein, followed by the execution of the Vina algorithm using the "run vina" option. The 2D and 3D interaction visualizations of the docked complexes were generated using Biovia Discovery Studio Visualizer (DSV) and PyMOL. PyMOL was employed for 3D structural visualization and active-site confirmation, while DSV was used to produce detailed 2D interaction diagrams, highlighting hydrogen bonds, hydrophobic contacts, and key amino acid interactions with MAO-B.

Docking validation was performed using re-docking of the co-crystallized ligand into the active site of the target protein (PDB ID: 2V5Z). The docked poses were compared with the crystallographic conformation using RMSD values calculated by AutoDock Vina. The top-ranked poses showed RMSD ≤ 2.0 Å (0.000 Å for best poses), confirming the accuracy and reliability of the docking protocol. Visualization and confirmation of binding interactions were performed using PyMOL and Discovery Studio Visualizer.

IN-SILICO ADME ANALYSIS AND DRUG-LIKENESS EVALUATION

The in silico ADME profiling and drug-likeness evaluation were conducted using the SwissADME web tool, developed by the Swiss Institute of Bioinformatics, available at www.swissadme.ch (35). Compounds with top-ranking binding energy scores were selected for this phase of the analysis. Basic physicochemical properties such as molecular weight (MW), molecular refractivity (MR), atom counts, and polar surface area (PSA) were calculated using OpenBabel, version 2.3.0 (36). Drug-likeness assessment was carried out using the rules of five (RO5) developed by Lipinski (2001), (37), Ghose (1999) (38), Veber (2002) (39), Egan (2000) (40), and Muegge (2001) (41). Abbot Bioavailability scores were calculated to estimate the likelihood of a compound achieving at least 10% oral bioavailability, based on total charge, TPSA, and Lipinski rule violations. Lipophilicity was evaluated using models such as iLOGP, XLOGP3, WLOGP, MLOGP, and SILICOS-IT, and a consensus log Po/w value was derived (35). Solubility (log S) predictions for the selected compounds were performed using three distinct models: ESOL, Ali (42, 43) and SILICOS-IT (35).

RESULTS

CAFFEINE ANALOGS AS MAO-B INHIBITORS

Caffeine and its derivatives are known MAO inhibitors, with compounds such as (E)-8-(3-chlorostyryl) caffeine and 8-(3-bromobenzyloxy) caffeine showing notable MAO-B inhibition (44). The chemical structures of reported MAO-B inhibitors are shown in Fig. 1. As a heterocyclic molecule, caffeine exhibits enhanced MAO-B inhibitory potential when substituted with phenyl alkyl groups at the C8 position. This study evaluated a series of C8-substituted caffeine analogues for their MAO-B inhibitory properties, with the binding affinities of all ligands summarized in Table II.

Table II. The binding energies of titled compounds

S. no.	Name of the compound	Binding affinities kcal/mol	H bonds	Hydrophobic interactions
1.	8-(2-Phenylethyl) caffeine (4a)	-9.9	Tyr 435	Leu171, Cys172, Ile199, Ile 316, Tyr 398
2.	8-(3- Phenylpropyl) caffeine (4b)	-9.9	Tyr 435	Leu171, Cys172, Ile199, Ile 316, Tyr 398, Tyr 326
3.	8-(4- Phenylbutyl) caffeine (4c)	-10.2	Tyr 435	Leu 164, Leu171, Cys172, Ile199, Ile 316, Tyr 398
4.	8-(5- Phenylpentyl) caffeine (4d)	-10.3	Tyr 435	Leu 164, Leu171, Cys172, Ile199, Ile 316, Tyr 398
5.	8-(6- Phenylhexyl) caffeine (4e)	-10.5	Pro 102, Pro104, Tyr 326	Leu 171, Ile 199, Ile 316, Tyr 398, Phe 343
6.	8-(7- Phenylheptyl) caffeine (4f)	-10.3	Pro 102, Pro104, Tyr 326	Leu 171, Ile 199, Ile 316, Tyr 398, Phe 343
7.	8-(3-Oxo-3-phenylpropyl) caffeine (4h)	-10.1	Ser 59, Lys 296, Tyr 398, Tyr435	Gly 57, Gly 58, Leu 171, Cys 172, Ile198, Trp 388, Cys 397
8.	8-(4-Oxo-4-phenylbutyl) caffeine (4i)	-10.3	Tyr 326, Tyr435	Leu 164, Leu171, Cys172, Ile199, Ile 316, Tyr 398

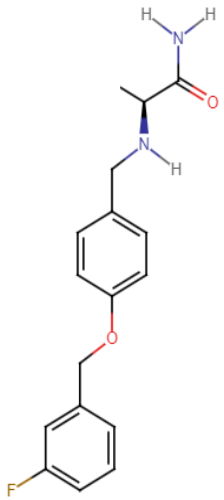

Safinamide

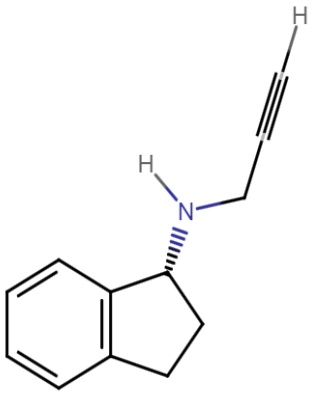

Rasagiline

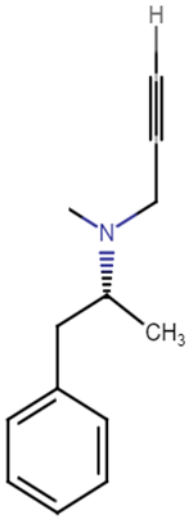

Selegiline

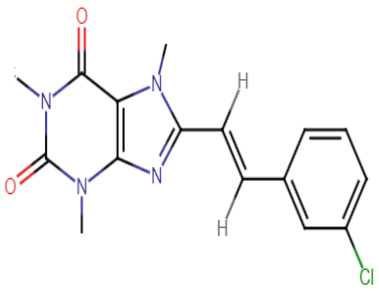

(E)-8-(3-Chlorostyryl)caffeine

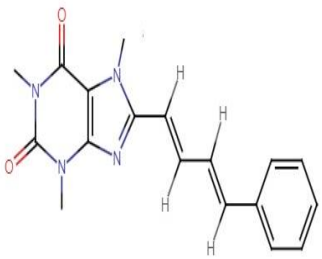

(E,E)-8-(4-Phenylbutadien-1-yl)caffeine

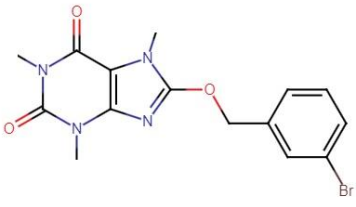

8-(3 bromobenzyloxy) caffeine

Fig. 1. Structure of reported inhibitors of MAO-B

DOCKING ANALYSIS

This study builds on a 2013 report (45) describing the synthesis and evaluation of a homologous series of C8-substituted caffeine derivatives, 4a–f and 4h, and 4i, bearing $-(CH_2)$□$-C_6H_5$ (n = 2–7) moieties and carbonyl-containing groups respectively. These compounds were investigated as human MAO-A and MAO-B inhibitors, revealing that variations in C8 chain length significantly influence MAO-B inhibitory potency and selectivity.

The docking analysis of 8-(2-phenylethyl) caffeine (4a) revealed key interactions with residues Leu171, Cys172, Ile199, Ile316, Tyr398, and Tyr435 of MAO-B. The ligand forms strong hydrogen and carbon–hydrogen bonds with the side chain of Tyr435, while two π–σ interactions are observed with Ile199 and Tyr398. Additionally, a π–π stacking interaction with Tyr398 and a π–alkyl interaction with Ile316 and Leu171 contribute to binding stability. Interaction with Cys172 further supports its affinity within the active site. These specific residue interactions highlight the ligand's selective binding to MAO-B. The 2D and 3D interaction models are shown in Fig. 2a.

The docking analysis of 8-(3-phenylpropyl) caffeine (4b) showed interaction patterns similar to those of 4a. A key hydrogen bond was formed between the side chain of Tyr435 and the ligand, accompanied by an additional carbon–hydrogen bond at the same site. The benzene ring of Tyr398 established both π–σ and π–π stacking interactions with the pyrimidine ring of 4b, while four π–alkyl interactions involved Leu171, Ile199, Ile316, and Tyr326. Additionally, Leu171 and Ile199 formed alkyl bonds at positions overlapping with their π–alkyl interactions, and Cys172 engaged in a π–sulfur bond with the imidazole ring of 4b. These interactions suggest that 4b binds selectively to MAO-B but with slightly weaker affinity than 4a, likely due to longer bond distances between the ligand and amino acid residues. The 2D and 3D interaction models are shown in Fig. 2b.

Ligands 8-(4-phenylbutyl) caffeine (4c) and 8-(5-phenylpentyl) caffeine (4d) displayed interaction patterns similar to 4b, differing mainly in bond lengths, which were shorter for 4d. Both formed hydrogen bonds with Tyr435 via the C6 oxygen atom and carbon–hydrogen bonds through the imidazole ring. Tyr398 participated in π–π stacking and π–σ interactions with the pyrimidine ring, positioning the caffeine core within the substrate cavity. Comparable π–alkyl interactions were observed with Leu171, Ile199, Ile316, and Tyr326, along with an additional π–alkyl interaction between the phenyl rings of 4c and 4d and Leu164. The molecular interactions are illustrated in Figs. 2c & d.

Earlier studies have shown that hydrophobic interactions mediated by phenyl rings are key to MAO-B binding and are generally more favorable than hydrogen or halogen bonds (46). Among the studied compounds, 4d demonstrated greater stability than 4a–4c, attributed to its strong hydrophilic interaction with Cys172 and enhanced hydrophobic contact via its phenyl ring, contributing to higher binding stability within the active site. Similarly, 8-(6-phenylhexyl) caffeine (4e) and 8-(7-phenylheptyl) caffeine (4f) exhibited comparable binding modes but with distinctive interaction patterns. In both, the phenyl ring and alkyl chain interact with residues in the substrate cavity, while the caffeine moiety extends toward the entrance cavity. These ligands form multiple van der Waals interactions with hydrophobic residues, along with carbon–hydrogen bonds involving Pro102, Pro104, and Tyr326. Their phenyl rings engage in π–π stacking with Tyr398, and additional π–alkyl interactions with Ile199, Ile316, Phe343, and Leu171 further stabilize the complex. The molecular interactions are illustrated in Figs. 2e & f.

Table III. Comparison of binding affinities (kcal/mol) of caffeine derivatives with standard reversible inhibitor safinamide

Compound	Binding affinity (kcal/mol)	Type of inhibition
4a	–9.9	Moderate
4b	–9.9	Moderate
4c	–10.0	Moderate
4d	–10.3	Strong
4e	–10.5	Strong
4f	–10.3	Strong

4h	–10.1	Moderate
4i	–10.2	Moderate
Safinamide (standard)	–9.8	Reversible

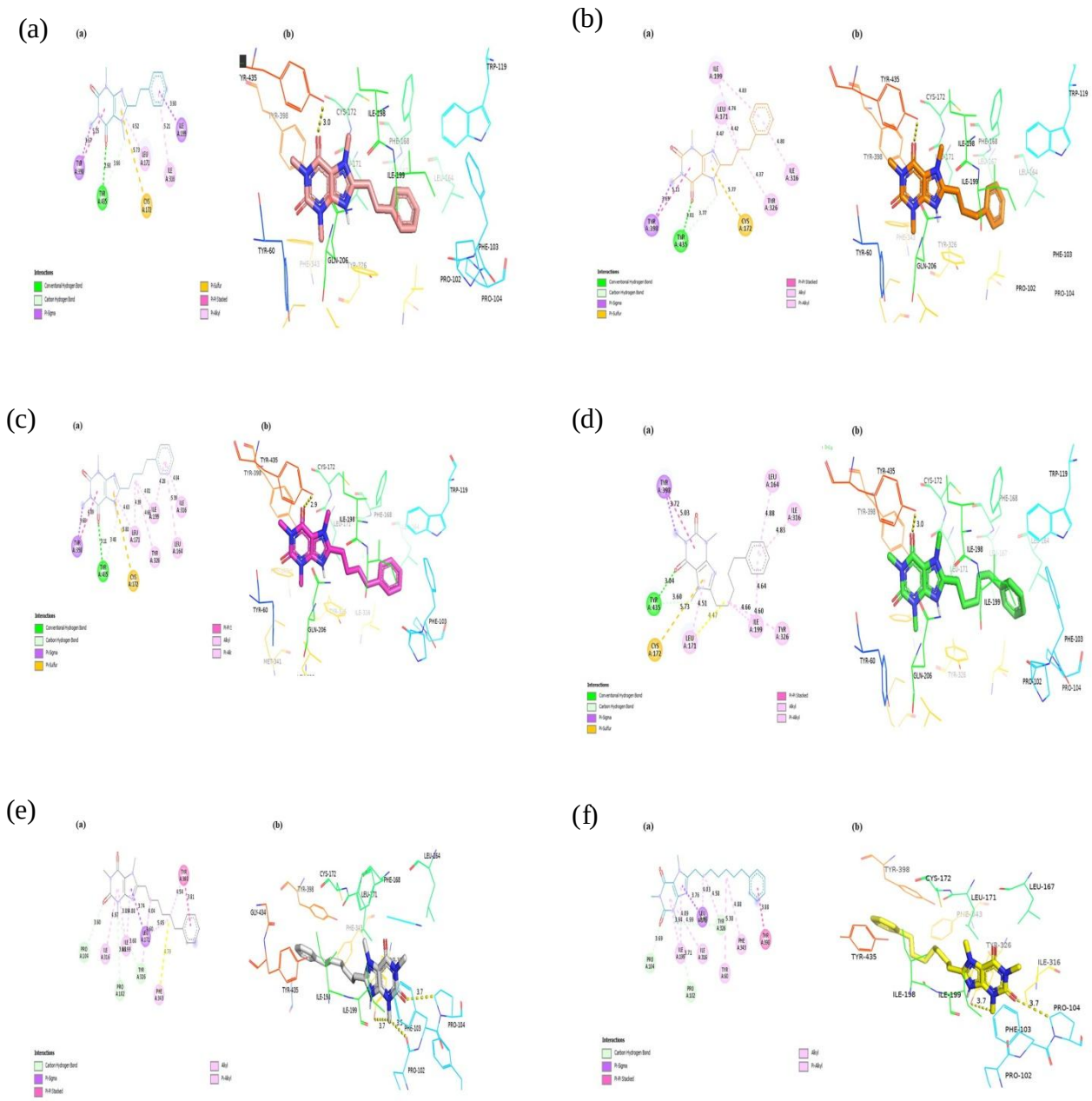

Fig. 2. Interaction models of C8-substituted caffeine analogues within the MAO-B binding site; **(a)**. Compound 4a; **(b).** Compound 4b (interacting residues; **(c).** compound 4c; **(d)** compound 4d; **(e)**. Compound 4e; **(f).** compound 4f. Conventional hydrogen bonds are shown as yellow dotted lines

These two ligands exhibit enhanced binding interactions due to their extended alkyl chains, which reach into the entrance cavity and establish additional van der Waals contacts with the protein. Previous studies have reported that C8-substituted caffeine derivatives preferentially bind within the hydrophobic region of MAO-B (47). Their selectivity for MAO-B over MAO-A arises from the structural restriction in MAO-A, where the non-rotatable residue Phe208 separates the substrate and entrance cavities, preventing larger inhibitors from fitting effectively (48).

The carbonyl-containing ligands 8-(3-oxo-3-phenylpropyl) caffeine (4h) and 8-(4-oxo-4-phenylbutyl) caffeine (4i) share structural similarity and were previously reported as weak MAO-B inhibitors with low IC_{50} values (45). Docking simulations, however, revealed distinct interaction profiles contributing to their

inhibitory potential. Among them, 4h exhibited moderate binding affinity toward MAO-B, forming hydrogen bonds with Ser59**,** Lys296, and Tyr435 via its carbonyl group. It also engaged in π–π stacking interactions with Tyr398 and Tyr435, a π–sulfur bond with Cys172 and Cys397, and π–alkyl interactions with Leu171 and Lys298. Additionally, 4h established a π–π T-shaped interaction with Trp388 and an amide–π stacking interaction with Gly57**.** Collectively, these interactions within the substrate cavity highlight the ligand's moderate yet specific binding behavior, as illustrated in Fig. 3a**.**

In contrast, 4i exhibited distinct outcomes from the reported inhibition study (45), revealing a favorable binding affinity towards the MAO-B enzyme. Its interactions closely resembled those observed in analogs 4a, 4b, 4c, and 4d. Notably, 4i established two conventional hydrogen bonds: one with Tyr326 involving t he carbonyl carbon of its oxo group, and another with Tyr435. Interactions with other amino acids, including Leu164, Leu171, Ile199, Ile316, and Tyr398, closely resembled those of the 4d analog, although the bond lengths exhibited variations (Fig. 3b). Interaction of the top-scored docking poses of phenyl alkyl derivatives with MAO-B is depicted in Fig. 3c.

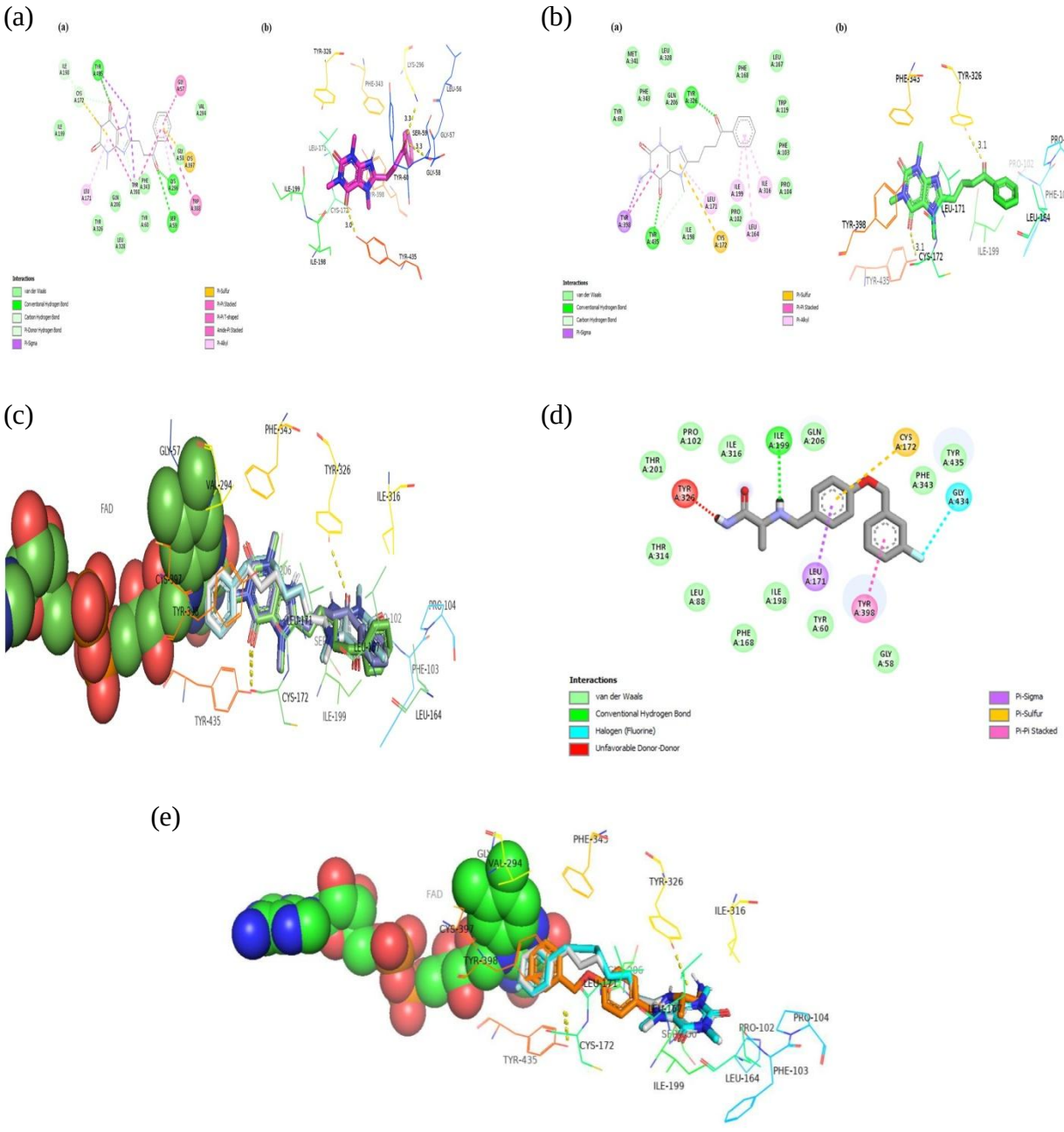

Fig. 3 (a). Intermolecular interactions between MAO-B and compound 4h; **(b)**. Interacting residues of compound 4b; **(c)**. Superimposed top-scored docking poses of derivatives 4d (light green), 4e (half white), 4f (light blue), and 4i (violet). Yellow dotted lines represent conventional hy drogen bonds; **(d).** Interaction of safinamide with MAO-B; **(e).** Comparison of safinamide with compound 4 f (light blue) and compound 4e (half white) in the MAO-B binding site

To validate the docking protocol and assess the relative binding performance of the phenyl alkyl caffeine derivatives, a comparative analysis was performed with the known MAO-B ligand safinamide. The standard reversible MAO-B inhibitor safinamide was docked against the MAO-B enzyme using the same parameters (AutoDock Vina via PyRx, grid box = 40 × 50 × 40 Å; exhaustiveness = 8). The docking results showed that safinamide exhibited a binding affinity of –9.8 kcal/mol, consistent with its reported reversible inhibition behavior. A comparative summary of binding energies for all C8-substituted caffeine derivatives with safinamide is presented in Table III. The longer-chain derivatives 4d, 4e, and 4f demonstrated stronger binding affinities (–10.3 to –10.5 kcal/mol) than safinamide, suggesting their potential as effective reversible MAO-B inhibitors. This provides further insights into the binding characteristics and similarities among these compounds. Our docking analysis revealed that safinamide interacts with key amino acid residues within the active site, including Leu 171, Cys 172, Ile 199, Tyr 326, and Tyr 398. This interaction pattern closely resembles that observed with our caffeine derivatives 4d and 4e, suggesting a consistent binding mode among these inhibitors. Fig. 3d depicts the interaction of safinamide with MAO-Band, Fig. 3e provides a comparison of safinamide with 4f and 4e in the MAO-B docking site. These analyses validate the docking approach and highlight the versatility of phenyl alkyl caffeine derivatives in achieving similar interactions with the MAO-B active site, thereby supporting their potential as effective MAO-B inhibitors.

MOLECULAR DOCKING SIMULATIONS FOR PHARMACOKINETICS, DRUG-LIKENESS, AND MEDICINAL CHEMISTRY PROPERTIES

For a compound to qualify as a viable drug candidate, it must demonstrate not only the desired biological activity but also favorable pharmacokinetic and safety profiles (49). Accordingly, selected compounds identified from the docking simulations were evaluated for their pharmacokinetic, drug-likeness, and medicinal chemistry properties using the SwissADME in silico tool. Lipophilicity, a key determinant of a compound's ADMET (absorption, distribution, metabolism, excretion, and toxicity) characteristics, reflects its ability to dissolve in lipid membranes and thus influences membrane permeability and bioavailability (50). Based on widely accepted drug-likeness criteria, such as Lipinski's rule of five, the optimal range of lipophilicity (log P) lies between 0 and 5, ensuring adequate solubility and permeability for oral drugs (37, 51).

The key physicochemical properties of the lead compounds identified through docking studies are summarized in Tables IV-VI. All compounds exhibited molecular weights below 500 g/mol (298.34–368.47 g/mol), consistent with favorable drug-like size and complexity. The fraction of sp^3 carbons increased from

Table IV. The fundamental physicochemical properties and computational descriptors of analysed compounds

Compounds	4a	4b	4c	4d	4e	4f	4h	4i
Log Po/w (iLOGP)	2.88	3.14	3.41	3.59	3.85	4.15	2.85	3.09
Log Po/w (XLOGP3)	1.82	2.18	2.72	3.26	3.80	4.34	1.18	1.54
Log Po/w (WLOGP)	0.76	1.15	1.54	1.93	2.32	2.71	0.79	1.18
Log Po/w (MLOGP)	2.22	2.47	2.70	2.94	3.16	3.39	1.60	1.83
Log Po/w (Silicos-IT)	1.78	2.15	2.54	2.93	3.33	3.72	1.70	2.09
Consensus Log Po/w	1.89	2.22	2.58	2.93	3.29	3.66	1.62	1.95

0.31 (4a) to 0.48 (4f), indicating greater molecular saturation and flexibility that may enhance biological interactions. The number of rotatable bonds rose from 3 (4a) to 8 (4f), reflecting increased conformational freedom in longer-chain derivatives. Topological polar surface area (TPSA) values were generally consistent, except for 4h and 4i, which showed higher TPSA, suggesting differences in solubility and permeability. Consensus log P values ranged from 1.62 (4h) to 3.66 (4f), with 4f being the most lipophilic, favoring membrane penetration but potentially reducing solubility. Accordingly, 4a and 4h were classified as soluble, while 4b–4e displayed moderate solubility, and 4f showed low solubility, which may affect its bioavailability. The ESOL log S values ranged from 2.81 (4h) to 4.74 (4f), consistent with these solubility trends.

Table V. Lipophilicity assessment of analyzed compounds

Compounds	4a	4b	4c	4d	4e	4f	4h	4i
ESOL log S	-3.14	-3.37	-3.71	-4.05	-4.40	-4.74	-2.81	-3.03
ESOL solubility mg/ml; mol/l	2.15e-01 7.20e-04	1.34e-01 4.28e-04	6.37e-02 1.95e-04	3.02e-02 8.86e-05	1.42e-02 4.01e-05	6.68e-03 1.81e-05	5.11e-01 1.57e-03	3.14e-01 9.24e-04
ESOL class	Soluble	Soluble	Soluble	Moderately soluble	Moderately soluble	Moderately soluble	Soluble	Soluble
Ali log S	2.74	-3.11	-3.67	-4.23	-4.79	-5.35	-2.43	-2.81
Ali solubility mg/ml; mol/l	5.45e-01 1.83e-03	2.42e-01 7.73e-04	6.95e-02 2.13e-04	1.99e-02 5.86e-05	5.71e-03 1.61e-05	1.63e-03 4.44e-06	1.21e+00 3.70e-03	5.32e-01 1.56e-03
Ali class	Soluble	Soluble	Soluble	Moderately soluble	Moderately soluble	Moderately soluble	Soluble	Soluble
Silicos-IT log S	-3.98	-4.38	-4.78	-5.17	-5.57	-5.96	-3.92	-4.31
Silicos-IT solubility mg/ml; mol/l	3.10e-02 1.04e-04	1.30e-02 4.16e-05	5.44e-03 1.67e-05	2.28e-03 6.70e-06	9.54e-04 2.69e-06	4.00e-04 1.09e-06	3.95e-02 1.21e-04	1.66e-02 4.86e-05
Silicos-IT class	Soluble	Moderately soluble	Moderately soluble	Moderately soluble	Moderately soluble	Moderately soluble	Soluble	Moderately soluble

Table VI. Predicted water solubility of analyzed compounds

Compounds	4a	4b	4c	4d	4e	4f	4h	4i
Formula	$C_{16}H_{18}N_4O_2$	$C_{17}H_{20}N_4O_2$	$C_{18}H_{22}N_4O_2$	$C_{19}H_{24}N_4O_2$	$C_{20}H_{26}N_4O_2$	$C_{21}H_{28}N_4O_2$	$C_{17}H_{18}N_4O_3$	$C_{18}H_{20}N_4O_3$
MW (g/mol)	298.34	312.37	326.39	340.42	354.45	368.47	326.35	340.38
No. heavy atoms	22	23	24	25	26	27	24	25
No. aromatic heavy atoms	15	15	15	15	15	15	15	15
Fraction Csp3	0.31	0.35	0.39	0.42	0.45	0.48	0.29	0.33
No rotatable bonds	3	4	5	6	7	8	4	5
No H-bond acceptors	3	3	3	3	3	3	4	4
No. H-bond donors	0	0	0	0	0	0	0	0
Molar Refractivity	86.30	91.11	95.91	100.72	105.53	110.33	91.53	96.33
TPSA	61.82 Å²	61.82 Å²	61.82 Å²	61.82 Å²	61.82 Å²	61.82 Å²	78.89 Å²	78.89 Å²

The pharmacokinetic analysis (Table VII) revealed that all compounds exhibited high gastrointestinal (GI) absorption, with 4b–4f showing effective BBB permeability, whereas 4a, 4h, and 4i did not. The absence of P-glycoprotein (P-gp) substrate properties indicates potential for improved therapeutic efficacy. However, inhibition of certain CYP enzymes suggests a possible risk of drug–drug interactions.

As shown in Table VIII, all compounds fulfilled drug-likeness criteria based on Lipinski's and related rules, demonstrating favorable oral bioavailability with a consistent drug-likeness score of 0.55. Compounds 4e and 4f, however, were not classified as lead-like due to higher molecular weights and lipophilicity, indicating that structural optimization may be required to improve their lead characteristics.

DISCUSSION

Caffeine is a widely consumed central nervous system stimulant, has been extensively studied for its potential as an MAO inhibitor. In this investigation, we aimed to elucidate the interaction and inhibitory effects of phenyl alkyl caffeine derivatives against MAO-B. Our results offer insights into the binding modes and interactions of phenyl alkyl C8 substituents of caffeine with the MAO-B enzyme at a molecular level. In this study, a series of phenyl alkyl caffeine analogs, namely 4a to 4i (excluding 4g due to its weak inhibitory effect), were subjected to docking analysis with the MAO-B protein.

Table VII. Predicted pharmacokinetic (ADME) profiles of analyzed compounds

Compounds	4a	4b	4c	4d	4e	4f	4h	4i
GI absorption	High	High	High	High	High	High	High	High
BBB permeant	No	Yes	Yes	Yes	Yes	Yes	No	No
P-gp substrate	No	No	No	No	No	No	No	No
CYP1A2 inhibitor	Yes	Yes	No	No	No	No	No	No
CYP2C19 inhibitor	Yes	Yes	Yes	Yes	Yes	Yes	No	Yes
CYP2C9 inhibitor	Yes	Yes	Yes	Yes	Yes	Yes	No	Yes
CYP2D6 inhibitor	No	No	No	No	No	No	No	No
CYP3A4 inhibitor	No	No	No	No	Yes	Yes	No	No
Log Kp [cm/s]	-6.83	-6.66	-6.36	-6.06	-5.76	-5.47	-7.45	-7.28

Table VIII. Predicted drug-likeness, medicinal chemistry, and lead-likeness attributes of analyzed compounds

Compounds	4a	4b	4c	4d	4e	4f	4h	4i
Lipinski	Yes;0 violation	Yes; 0 violation	Yes; 0 violation	Yes;0 violation	Yes;0 violation	Yes; 0 violation	Yes; 0 violation	Yes; 0 violation
Ghose	Yes	Yes	Yes	Yes	Yes	Yes	Yes	Yes
Veber	Yes	Yes	Yes	Yes	Yes	Yes	Yes	Yes
Egan	Yes	Yes	Yes	Yes	Yes	Yes	Yes	Yes
Muegge	Yes	Yes	Yes	Yes	Yes	Yes	Yes	Yes
Bioavailability score	0.55	0.55	0.55	0.55	0.55	0.55	0.55	0.55
PAINS	0 alert	0 alert	0 alert	0 alert	0 alert	0 alert	0 alert	0 alert
Brenk	0 alert	0 alert	0 alert	0 alert	0 alert	0 alert	0 alert	0 alert
Leadlikeness	Yes	Yes	Yes	Yes	No; 2 violations: MW>350, XLOGP3>3.5	No; 3 violations: MW>350, Rotors>7, XLOGP3>3.5	Yes	Yes
Synthetic accessibility	2.72	2.80	2.89	3.01	3.12	3.23	2.75	2.83

The findings of this study are consistent with previous reports on caffeine analogues and MAO-B inhibitors. Earlier studies have demonstrated that C8-substituted caffeine derivatives, particularly those incorporating extended hydrophobic or aromatic side chains, exhibit enhanced inhibitory potency and selectivity toward MAO-B by effectively occupying both the substrate and entrance cavities of the enzyme's active site (52, 53). In agreement with these observations, the present work revealed that derivatives 4d, 4e, and 4f, containing longer phenyl alkyl chains, showed robust binding affinities with –10.3 to –10.5 kcal/mol energy values, respectively, than shorter-chain analogues. This pattern aligns with the structure–activity relationships reported by Petzer and colleagues, who found that increasing alkyl chain length enhances MAO-B selectivity and reversibility (52). Moreover, the docking performance of these derivatives was comparable or superior to that of safinamide, which demonstrated a binding affinity of –9.8 kcal/mol, a clinically established reversible MAO-B inhibitor (26), further supporting their potential as selective and reversible MAO-B inhibitors suitable for therapeutic exploration in neurodegenerative disorders. It is important to note that MAO-B's active sites consist of two distinct cavities, namely the substrate and entrance cavities. Our analysis suggested that all the inhibitors first entered through the entrance cavity before exerting their effects within the substrate cavity. For larger inhibitors, such as those observed in 4d,

4e, and 4f, previous studies noticed that the amino acid Ile 199 rotated. This rotation helps these larger molecules fit into the entrance cavity by merging two cavities (54). The molecular interaction analysis for 4d, 4e, 4f, and 4i revealed their extended binding characteristics within the hydrophobic region of the entrance cavity.

Conversely, analogs with shorter substituents, including 8-(2-Phenylethyl) caffeine (4a), 8-(3-Phenylpropyl) caffeine (4b), 8-(4-Phenylbutyl) caffeine (4c), and 8-(3-Oxo-3-phenylpropyl) caffeine (4h), displayed moderate interactions with the amino acids in the substrate cavity of MAO-B. The shorter phenyl alkyl C8 substituents, including 4a, 4b, 4c, and 4h, engaged with amino acid residues within the substrate cavity. Due to their relatively shorter alkyl chain length, these analogs exhibited moderate binding energies. 8-(5-Phenylpentyl) caffeine (4d) emerged as the most selective inhibitor, as reported by Petzera et al (45). Molecular interaction analysis highlighted its selective binding within active site amino residues, characterized by moderate bond lengths and more pronounced hydrophobic interaction with its phenyl ring.

Both 8-(6-Phenylhexyl) caffeine (4e) and 8-(7-Phenylheptyl) caffeine (4f) demonstrated compelling binding affinities, with 4e exhibiting the best affinity among all inhibitors. These two inhibitors shared similar binding interactions; their caffeine moieties were positioned within the entrance cavity. However, a key difference between them was in their IC50 values, where 4f displayed reversibility as mentioned earlier. 4e displayed a greater level of selectivity in comparison to 4f (45). 8-(4-Oxo-4-phenylbutyl) caffeine (4i), showcased favorable binding energy due to strong molecular interactions, involving two strong conventional hydrogen bonds. Despite its strong interactions, 4i might not be as efficacious, as it displayed lower IC50 and Selectivity Index values (45).

In contrast, we observed weaker binding energies for 4a (-9.9 kcal/mol), 4b (-9.9 kcal/mol), and 4h (-10.1 kcal/mol). Remarkably, 4h, despite establishing three conventional hydrogen bonds, exhibited weak molecular interactions that involved unnecessary amino acid residues rather than direct interactions with active site amino acids. Analogs 4a, 4b, and 4c exhibited moderate binding within the active site, typically involving a single conventional hydrogen bond.

The analyzed MAO-B inhibitors exhibit promising physicochemical and pharmacokinetic properties, making them suitable candidates for further development in the treatment of Parkinson's disease. For central nervous system (CNS) drugs, ensuring both BBB permeability and GI absorption is essential for therapeutic success. As tightly regulated between the bloodstream and the brain, the blood-brain barrier limits the entry of most compounds and drugs (55). Physicochemical properties, such as lipophilicity, molecular size, the number of hydrogen bonds, and active transport/efflux systems, influence passage at the BBB. Lacking adequate properties, systemic administration may result in insufficient brain exposure and treatment failure (56). Ultimately, brain exposure depends on good GI absorption or effective uptake into the systemic circulation. This drug's bioavailability depends on drug dissolution, stability in the GI tract, permeability across the intestinal epithelium, first-pass metabolism, GI transit time, and other physiological factors after oral administration. Maximizing GI absorption is crucial to crossing the BBB and reaching the brain target for CNS therapeutics (57). The consistency in high GI absorption across all compounds suggests that they can be effectively delivered orally. The ability of certain compounds to penetrate the BBB is critical for targeting the central nervous system, which is essential for treating neurodegenerative disorders. The variation in lipophilicity among the compounds points to optimizing these properties to enhance solubility and permeability, particularly for those with lower consensus log P values. The solubility data indicate a potential limitation for some compounds that could affect their bioavailability and therapeutic efficacy. The lack of alerts in PAINS and Brenk screening suggests that these compounds do not exhibit structural motifs associated with undesirable side effects, indicating their potential for safer therapeutic profiles. However, the CYP inhibition profiles should be carefully considered in drug development, as interactions with other medications may affect the therapeutic outcome.

Although in vitro MAO-B inhibition assays with IC_{50} determination have been performed for the selected caffeine derivatives (45), additional studies are required to further validate and extend these

findings. Enzyme kinetics studies should be performed to elucidate their mechanism and the reversibility of inhibition. Furthermore, cell-based assays can assess neuroprotective potential, cytotoxicity, and selectivity over MAO-A, while in vivo models of Parkinson's disease could provide critical insights into their pharmacodynamic efficacy, BBB permeability, and safety profiles. Collectively, these studies would offer a robust experimental foundation supporting the therapeutic potential of the identified MAO-B inhibitors.

CONCLUSION

The research highlights the significant MAO-B inhibitory potential of longer phenyl alkyl caffeine derivatives, which uniquely interact with the MAO-B active site through the rotation of amino acid Ile199. Shorter substituents show moderate substrate cavity interactions, whereas 8-(5-Phenylpentyl) caffeine (4d) emerges as a selective inhibitor. Both 8-(6-Phenylhexyl) caffeine (4e) and 8-(7-Phenylheptyl) caffeine (4f) exhibit strong binding affinity, with 4e demonstrating high selectivity and 4f showing reversible inhibition. Importantly, these compounds preferentially inhibit MAO-B over MAO-A. Although 8-(4-Oxo-4phenylbutyl) caffeine (4i) shows robust interactions, it may have some limitations requiring further study. These findings advance the understanding of caffeine derivatives as promising MAO-B inhibitors with therapeutic potential for neurological disorders. ADME analysis reveals that compounds 4b, 4c, 4d, 4e, and 4f possess favorable pharmacokinetic properties, including good blood-brain barrier permeability and high gastrointestinal absorption, making them strong candidates for neurodegenerative disease treatment. In contrast, compounds 4a, 4h, and 4i may need optimization to improve CNS penetration. Among all, compound 4f stands out as the most promising ligand based on its overall ADME profile and inhibitory characteristics. Hence, this study provides valuable structural insights and pharmacokinetic data supporting the development of phenyl alkyl caffeine derivatives as selective, potent, and drug-like MAO-B inhibitors for potential use in managing neurodegenerative conditions.

Author's Contributions:

UJ & AF Conducted material preparation, data analysis and writing of the manuscript; AF Drafted and finalized the complete manuscript, including data collection and analysis; SB Investigated, wrote and edited the manuscript; TF Data curation and preparation of materials.

Declaration of generative AI-Assisted Tools:

No AI-assisted tools were used.

Conflict of Interest:

The authors report no conflicts of interest.

References:

1. Shahid R, Begum S. A New Insight in Cellular and Molecular Signaling Regulation for Neural Differentiation Program. Molecular neurobiology. 2025;20:1-22.
2. Youdim MB, Edmondson D, Tipton KF. The therapeutic potential of monoamine oxidase inhibitors. Nature reviews neuroscience. 2006;7(4):295-309.
3. Nebbioso M, Pascarella A, Cavallotti C, Pescosolido N. Monoamine oxidase enzymes and oxidative stress in the rat optic nerve: age-related changes. International journal of experimental pathology. 2012;93(6):401–5.
4. Huang M, Xie SS, Jiang N, Lan JS, Kong LY, Wang XB, Wang. Multifunctional coumarin derivatives: monoamine oxidase B (MAO-B) inhibition, anti-β-amyloid (Aβ) aggregation and metal chelation properties against Alzheimer's disease. Bioorganic and medicinal chemistry letters. 2015;25(3):508–13.
5. Noda S, Sato S, Fukuda T, Tada N, Uchiyama Y, Tanaka K, Hattori N. Loss of Parkin contributes to mitochondrial turnover and dopaminergic neuronal loss in aged mice. Neurobiology of disease. 2020;136:104717.
6. Youdim MB, Bakhle YS. Monoamine oxidase: isoforms and inhibitors in Parkinson's disease and depressive illness. British journal of pharmacology. 2006;147(Suppl 1):S287–96.

7. Tetrud JW, Koller WC. A novel formulation of selegiline for the treatment of Parkinson's disease. Neurology. 2004;63(7 Suppl 2):S2–6.
8. Carradori S, D'Ascenzio M, Chimenti P, Secci D, Bolasco A. Selective MAO-B inhibitors: a lesson from natural products. Molecular diversity. 2014;18(1):219–43.
9. Chandran N, Lee J, Prabhakaran P, Kumar S, Sudevan ST, Parambi DG, Alsahli TG, Pant M, Kim H, Mathew B. New class of thio/semicarbazide-based benzyloxy derivatives as selective class of monoamine oxidase-B inhibitors. Scientific reports. 2024;14(1):31292.
10. Parkinson Study Group. Effect of deprenyl on the progression of disability in early Parkinson's disease. New England journal of medicine. 1989;321(21):1364–71.
11. Poewe W, Seppi K, Fitzer-Attas CJ, Wenning GK, Gilman S, Low PA, Giladi N, Barone P, Sampaio C, Eyal E, Rascol O. Efficacy of rasagiline in patients with the parkinsonian variant of multiple system atrophy: a randomised, placebo-controlled trial. The lancet neurology. 2015;14(2):145-52.
12. Khanam S, Subitsha AJ, Sabu S. Plants as a promising source for the treatment of Parkinson disease: a systematic review. International journal of comprehensive and advanced pharmacology. 2021;5(3):158–66.
13. Tipton KF, Boyce S, O'Sullivan J, Davey GP, Healy J. Monoamine oxidases: certainties and uncertainties. Current medicinal chemistry. 2004;11(15):1965–82.
14. Fowler JS, Volkow ND, Logan J, Wang GJ, MacGregor RR, Schlyer D. Slow recovery of human brain MAO B after L-deprenyl (Selegiline) withdrawal. Synapse. 1994;18(1):86–93.
15. Alborghetti M, Bianchini E, De Carolis L, Galli S, Pontieri FE, Rinaldi D. Type-B monoamine oxidase inhibitors in neurological diseases: clinical applications based on preclinical findings. Neural regeneration research. 2024;19(1):16-21.
16. Smellie FW, Davis CW, Daly JW, Wells JN. Alkylxanthines: inhibition of adenosine-elicited accumulation of cyclic AMP in brain slices and of brain phosphodiesterase activity. Life sciences. 1979;24(26):2475–82.
17. Boulenger JP, Patel J, Marangos PJ. Effects of caffeine and theophylline on adenosine and benzodiazepine receptors in human brain. Neuroscience letters. 1982;30(3):161–6.
18. Vlok N, Malan SF, Castagnoli N Jr, Bergh JJ, Petzer JP. Inhibition of monoamine oxidase B by analogues of the adenosine A2A receptor antagonist (E)-8-(3-chlorostyryl) caffeine (CSC). Bioorganic and medicinal chemistry. 2006;14(11):3512–21.
19. Strydom B, Malan SF, Castagnoli N Jr, Bergh JJ, Petzer JP. Inhibition of monoamine oxidase by 8-benzyloxycaffeine analogues. Bioorganic and medicinal chemistry. 2010;18(3):1018–28.
20. Pretorius J, Malan SF, Castagnoli N Jr, Bergh JJ, Petzer JP. Dual inhibition of monoamine oxidase B and antagonism of the adenosine A2A receptor by (E, E)-8-(4-phenylbutadien-1-yl) caffeine analogues. Bioorganic and medicinal chemistry. 2008;16(19):8676–84.
21. Mateev E, Kondeva-Burdina M, Georgieva M, Zlatkov A. Repurposing of FDA-approved drugs as dual-acting MAO-B and AChE inhibitors against Alzheimer's disease: an in silico and in vitro study. Journal of molecular graphics and modelling. 2023;122:108471.
22. Alagöz MA, Oh JM, Zenni YN, Özdemir Z, Abdelgawad MA. Development of a novel class of pyridazinone derivatives as selective MAO-B inhibitors. Molecules. 2022;27(11):3801.
23. Venkidath A, Oh JM, Dev S, Amin E, Rasheed SP, et al. Selected class of enamides bearing nitro functionality as dual-acting with highly selective monoamine oxidase-B and BACE1 inhibitors. Molecules. 2021;26(19):6004.
24. Binda C, Newton-Vinson P, Hubálek F, Edmondson DE, Mattevi A. Structure of human monoamine oxidase B, a drug target for the treatment of neurological disorders. Nature structural biology. 2002;9(1):22–6.
25. Binda C, Wang J, Pisani L, Caccia C, Carotti A, Salvati P. Structures of human monoamine oxidase B complexes with selective noncovalent inhibitors: safinamide and coumarin analogs. Journal of medicinal chemistry. 2007;50(24):5848–52.
26. Mostert S, Petzer A, Petzer JP. Indanones as high-potency reversible inhibitors of monoamine oxidase. Chem Med Chem. 2015;10(5):862–73.
27. Edmondson DE, Binda C, Mattevi A. Structural insights into the mechanism of amine oxidation by monoamine oxidases A and B. Archives of biochemistry and biophysics. 2007;464(2):269–76.
28. Fonseca A, Reis J, Silva T, Matos MJ, Bagetta D, Ortuso F. Coumarin versus chromone monoamine oxidase B inhibitors. Journal of medicinal chemistry. 2017;60(18):7206–12.
29. Mateev E, Georgieva M, Mateeva A, Zlatkov A, Ahmad S, Raza K, Azevedo V, Barh D. Structure-based design of novel MAO-B inhibitors: a review. Molecules. 2023;28(12):4814.

30. Shahwan M, Prasad P, Yadav DK, Altwaijry N, Khan MS, Shamsi A. Identification of high-affinity Monoamine oxidase B inhibitors for depression and Parkinson's disease treatment: bioinformatic approach of drug repurposing. Frontiers in pharmacology. 2024;15:1422080.
31. Binda C, Wang J, Pisani L, Caccia C, Carotti A, Salvati P, Edmondson DE, Mattevi A. Structures of human monoamine oxidase B complexes with selective reversible inhibitors. Biochemistry. 2011;50(23):5846–5852.
32. Yau MQ, Loo JS. Consensus scoring evaluated using the GPCR-Bench dataset: reconsidering the role of MM/GBSA. Journal of computer-aided molecular design. 2022; 36(5):427–41.
33. Sahakyan H. Improving virtual screening results with MM/GBSA and MM/PBSA rescoring. Journal of computer-aided molecular design. 2021;35(6):731–6.
34. BIOVIA, Dassault Systèmes. Discovery Studio modeling environment, release 2021. San Diego: Dassault systèmes; 2021.
35. Daina A, Michielin O, Zoete V. SwissADME: a free web tool to evaluate pharmacokinetics, drug-likeness, and medicinal chemistry friendliness of small molecules. Scientific reports. 2017;7:42717.
36. O'Boyle NM, Banck M, James CA, Morley C, Vandermeersch T, Hutchison GR. Open Babel: an open chemical toolbox. Journal of cheminformatics. 2011;3:33.
37. Lipinski CA, Lombardo F, Dominy BW, Feeney PJ. Experimental and computational approaches to estimate solubility and permeability in drug discovery and development settings. Advanced drug delivery reviews. 2001;46(1–3):3–26.
38. Ghose AK, Viswanadhan VN, Wendoloski JJ. A knowledge-based approach in designing combinatorial or medicinal chemistry libraries for drug discovery. Journal of combinatorial chemistry. 1999;1(1):55–68.
39. Veber DF, Johnson SR, Cheng HY, Smith BR, Ward KW, Kopple KD. Molecular properties that influence the oral bioavailability of drug candidates. Journal of medicinal chemistry. 2002;45(12):2615–23.
40. Egan WJ, Merz KM, Baldwin JJ. Prediction of drug absorption using multivariate statistics. Journal of medicinal chemistry. 2000;43(15):3867–77.
41. Muegge I, Heald SL, Brittelli D. Simple selection criteria for drug-like chemical matter. Journal of medicinal chemistry. 2001; 44(12):1841–6.
42. Delaney JS. ESOL: estimating aqueous solubility directly from molecular structure. Journal of Chemical information and computer sciences. 2004;44(3):1000–5.
43. Ali J, Camilleri P, Brown MB, Hutt AJ, Kirton SB. Revisiting the general solubility equation: in silico prediction of aqueous solubility incorporating the effect of topographical polar surface area. Journal of chemical information and modeling. 2012;52(2):420–8.
44. Van den Berg D, Zoellner KR, Ogunrombi MO, Malan SF, Terre'Blanche G, Castagnoli N Jr. Inhibition of monoamine oxidase B by selected benzimidazole and caffeine analogues. Bioorganic and medicinal chemistry. 2007;15(11):3692–702.
45. Petzer A, Grobler P, Bergh JJ, Petzer JP. Inhibition of monoamine oxidase by selected phenyl alkyl caffeine analogues. Journal of pharmacy and pharmacology. 2014;66(5):677–87.
46. Rauhamäki S, Postila PA, Niinivehmas S, Kortet S, Schildt E, Pasanen M. Structure–activity relationship analysis of 3-phenylcoumarin-based monoamine oxidase B inhibitors. Frontiers in chemistry. 2018; 6:41.
47. Strydom B, Malan SF, Castagnoli N Jr, Bergh JJ, Petzer JP. Inhibition of monoamine oxidase by 8-benzyloxycaffeine analogues. Bioorganic and medicinal chemistry. 2010;18(3):1018–1028.
48. Son SY, Ma J, Kondou Y, Yoshimura M, Yamashita E, Tsukihara T. Structure of human monoamine oxidase A at 2.2-Å resolution: the control of opening the entry for substrates/inhibitors. Proceedings of the national academy of sciences of the United States of America. 2008;105(15):5739–44.
49. Hu Q, Feng M, Lai L, Pei J. Prediction of drug-likeness using deep autoencoder neural networks. Frontiers in genetics. 2018; 9:511.
50. Arnott JA, Planey SL. The influence of lipophilicity in drug discovery and design. Expert opinion on drug discovery. 2012;7(9):863–75.
51. Waring MJ. Lipophilicity in drug discovery. Expert opinion on drug discovery. 2010; 5(3):235–48.
52. Petzer, JP, Castagnoli KP, Steyn S, Bergh JJ, Castagnoli, N. Inhibition of monoamine oxidase B by 8-benzyl caffeine analogues. Bioorganic and medicinal chemistry letters. 2013; 23(2):520–523.
53. Ramsay, R. R., & Albreht, A. Biochemical and structural characterization of MAO inhibitors for Parkinson's disease therapy. Frontiers in pharmacology. 2017; 8**:** 436.

54. Hubálek F, Binda C, Khalil A, Li M, Mattevi A, Castagnoli N, Edmondson DE. Demonstration of isoleucine 199 as a structural determinant for the selective inhibition of human monoamine oxidase B by specific reversible inhibitors. Journal of biological chemistry. 2005;280(17):15761–6.
55. Whelan R, Hargaden GC, Knox AJ. Modulating the blood–brain barrier: a comprehensive review. Pharmaceutics. 2021;13(11):1980.
56. Kadry H, Noorani B, Cucullo L. A blood-brain barrier overview on structure, function, impairment, and biomarkers of integrity. Fluids and barriers of CNS. 2020;17(1):69.
57. Abuhelwa AY, Williams DB, Upton RN, Foster DJ. Food, gastrointestinal pH, and models of oral drug absorption. European journal of pharmaceutics and biopharmaceutics. 2017;112:234-48.